Electronic Journal of Biotechnology 80 (2026) 100705

Contents lists available at ScienceDirect

Electronic Journal of Biotechnology

journal homepage: www.elsevier.com/locate/ejbt

Research article

Systems-level analysis prioritizes the importance of IFNG, SULF1, and OAS3 genes in head and neck cancer ☆

Juweria Khawar [a], Jinlei Guo [b], Saeed Akhtar [c], Baogang Bai [d,e,f], Syed Aun Muhammad [a,*]

[a] Institute of Molecular Biology and Biotechnology, Bahauddin Zakariya University Multan, 60800, Pakistan
[b] School of Intelligent Medical Engineering, North Henan Medical University, Xinxiang, Henan, China
[c] Multan Institute of Nuclear Medicine & Radiotherapy (MINAR), Multan, Pakistan
[d] School of Information and Technology, Wenzhou Business College, Wenzhou, Zhejiang, China
[e] Zhejiang Province Engineering Research Center of Intelligent Medicine, Wenzhou, Zhejiang, China
[f] The 1st School of Medical, School of Information and Engineering, The 1st Affiliated Hospital of Wenzhou Medical University, Zhejiang, China

GRAPHICAL ABSTRACT

Systems-level analysis prioritizes the importance of IFNG, SULF1, and OAS3 genes in head and neck cancer.

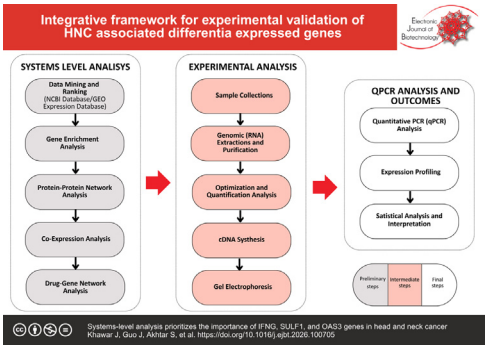

ARTICLE INFO

Article history:
Received 4 August 2025
Accepted 8 January 2026
Available online 5 February 2026

Keywords:
Differentially expressed genes
Enrichment analysis
Functional genomics
Gene expression profiling
Head cancer
HNC
Neck cancer

ABSTRACT

Background: Head and neck cancer (HNC) is one of the most prevalent and challenging diseases affecting a large population worldwide. Functional genomics can help understand the disease, but expressed gene therapy is uncertain. The study sought to identify specific genetic mutations and protein expression profiles in HNC.

Results: We ranked IFNG, SULF1, and OAS3 as three HNC-related genes ($p < 0.05$) based on the data mining. N-acetyleglucosamine-6-sulfatase activity, arylsulfatase, 2,5-oligoadenylate synthetase activity, interferon-gamma receptor binding, and other essential biological processes were all significantly correlated with the gene ontology (GO) terms. Nucleotide excision repair pathways, RNA polymerase-I transcription start and termination, RNA polymerase-II promoter escape, pyrimidine biosynthesis, and interferon-gamma signaling were all linked in the pathway enrichment. OAS1, IFIT1, CD4, STAT3, NFKBIA, RIPK1, SLCO5A1, and others are functionally connected to the co-expressed genes, while COL3A1 and SCEL are indirectly linked. Compared to controls, the quantitative PCR (qPCR) of these genes

☆ Audio abstract available in Supplementary material.

Peer review under responsibility of Pontificia Universidad Católica de Valparaíso.

* Corresponding author.
E-mail address: aunmuhammad78@yahoo.com (S.A. Muhammad).

https://doi.org/10.1016/j.ejbt.2026.100705

Pathway enrichment analysis
Personalized medicine
RT-qPCR

showed a significant two-fold change (FC) expression (2^{-DDC}_{T}) pattern of SULF1 (FC ≤ 1.2), OAS3 (FC ≤ 0.13), and IFNG (FC ≤ 0.12) compared to reference gene GAPDH (FC = 1). Pathophysiological cancer development is associated with up- and downregulated expression of these genes. The study found that personalized medicine can improve HNC treatment by adapting medication to each patient's tumor's molecular traits.
Conclusions: A substantial correlation between the pathophysiology of HNC and the *IFNG, SULF1*, and *OAS3* genes is found. This research could expedite the progress of drug discovery and aid in modifying HNC's treatment approaches.
How to cite: Khawar J, Guo J, Akhtar S, et al. Systems-level analysis prioritizes the importance of IFNG, SULF1, and OAS3 genes in head and neck cancer. Electron J Biotechnol 2026;80. https://doi.org/10.1016/j.ejbt.2026.100705.

1. Introduction

Head and neck cancer (HNC) is one of the most prevalent malignant diseases [1,2], and it is the fifth largest cause of death globally [3]. It accounts for 30% of all cancer-related mortality. HNC is not a localized cancer, and there are various types depending on the location of its origin. It is a multifactorial disease [4] associated with multiple risk factors. There are various contributing factors to the disease, including consumption of smoking or smokeless tobacco, which is a known risk factor for the condition as mentioned earlier [5]. Any abnormalities could raise the risk of a number of illnesses, including cancer. The most significant risk factors for HNC are psychological variables, primarily long-term tobacco use, alcoholism, and Epstein-Barr virus or human papillomavirus infection. Because these substances have the potential to harm DNA, cells need to activate the proper pathways in order to operate properly. Genomic instability is a characteristic of cancer cells that is linked to enhance a higher potential for DNA damage deposition. Numerous researches have evaluated the relationship between polymorphisms in DNA repair genes and a higher probability of head and neck cancer. So, patient's culture and risk factors have an impact on how polymorphisms in genes that repair DNA contribute to the liability to HNC. These genetic variants need to be further identified [6]. In low-income countries, the lifestyle and addictive behavior of betel use, gutka use, and beverages play a substantial role in disease etiology [7]. Another risk factor is a familial history of cancer that makes HNC vulnerable [8]. The computational study correlations and patterns that can be used to make predictions using methods that were developed to identify tumor cases. AlphaFold, an artificial intelligence tool from Google DeepMind, can show changes in DNA and forecast protein structures. Sequencing technologies, particularly next-generation sequencing (NGS), have been extensively employed in clinical and scientific applications [9]. This application offers information about possible illness risks and forecasts how genetic alterations may impact the protein environment. Other programs, like DeepMind's AlphaMissense, are being used to predict genetic illnesses. Using techniques like a thorough analysis of genetic variations and precise interpretation, modern automated programs seek to provide precise facts about mutations that cause disease. These procedures are crucial for figuring out the prevalence of specific illnesses using early identification and preventative techniques. Additionally, these procedures assist physicians in assessing the severity of the illness, choosing the best course of action for each patient, and enhancing patient outcomes. In order to effectively and efficiently evaluate disease, doctors and other healthcare professionals need to be able assess genetic risks [10]. Chemotherapeutic and targeted drugs, such as 5-fluorouracil and platinum analogs, are currently the primary approaches used to increase the effectiveness of radiotherapy [6,7]. Yet a number of preclinical and clinical research studies indicated that these chemotherapy agents were not more effective than radioactive therapy alone [8,9]. Targeted drugs are attracting significant recognition as alternative radioactive substances because of their notable effectiveness, accurate administration, and minimal adverse reactions [11]. Although therapeutic options have been improved, the prognosis remains dismal [12]. Genetic variations are associated with regulatory control factors, including DNA-repairing genes, cell cycle, aging, and cell death. Non-repaired DNA results in mutations of genes and genomic instabilities leading to HNC. Various studies have shown the importance of many genes in cancer progression and development. Most genes implicated in HNC are reported to be significant therapeutic targets, but their interactions and the complexities involved in developing effective therapies remain poorly understood [4].

Molecular dynamics simulation and drug molecular docking are examples of traditional molecular design techniques that operate by closely examining the mapping of structures to molecular properties. These kinds of trial-and-error-based molecular design techniques are frequently expensive and ineffective. On the other hand, by mapping attributes to structures, the inverse design of molecules infers molecules by prespecifying the properties of target molecules. Recent methodologies for studying the substantial role of functional genes in HNC have identified a regulatory role in cell cycles. However, the functional annotation of these genes is not fully understood, and there is a scientific gap between genetics and clinical outcomes, and therefore, the scientists are working to fix these challenges. Predicting important features from the functional level can successfully lessen the negative impacts of heterogeneity and produce more repeatable and comprehensible biomarkers. Genes typically interact with one another as functional modules to play synergistic roles. Pathways comprise a specific number of molecules whose interactions will realize particular activities, and they can reflect biological processes in cells, such as biological metabolism, signal transmission, and growth cycle [13]. It is observed that the *SULF1* polymorphism is associated with a variety of malignancies, including breast cancer, pancreatic carcinoma, and renal cancer. It implies that abnormalities of this gene are substantially more common in cancer pathophysiology. Similarly, abnormal expression of *OAS3* and *GTF2H4*, regulatory and DNA-repairing genes, is linked to a variety of cancer types, including sarcomas, colorectal carcinogenesis, and breast cancer [14,15]. *IFNG* is another vital gene that is an anti-proliferative, antiviral, and anti-tumor effector, and its abnormalities are related to TSC2 angiomyolipoma, a renal modifier of hepatitis C virus [16]. Other genes, including *DUT* and *EVER1*, play an important part in the nucleic acid metabolic pathways affecting DNA replication and are linked to a variety of cancers.

To determine HNC's genetic etiology, real-time quantitative PCR (RT-qPCR) was used to compare patient and control expression patterns. This approach is effective for expression profiling and studying the association with the HNC. 2^{-DDC}_{T} is a significant

application for calculating relative gene expression in qPCR analysis. This method is still effective for assessing the differential expression of transcripts between several patients by directly measuring the threshold cycle (C_T).

This system-level framework using biological networks may help to identify crucial etiological molecular entities of cancer. The goal of this study is to examine (1) the functional association of various genes in cancer, (2) phenomics to reactomic-level analysis, and (3) differential analysis and expression profiling among cases and controls. These outcomes will help to understand the genetic basis of the disease and to change the therapeutic options for head and neck cancer.

2. Materials and methods

2.1. Ethical approval

We collected blood samples of 100 individuals with an equal number of controls and cases from the Multan Institute of Nuclear Medicine and Radiotherapy, Multan (MINAR). The informed consent from individuals (cases and controls) was obtained for experimentation. This study was carried out in accordance with the Code of Ethics of the World Medical Association for experiments involving humans. Samples were obtained based on inclusion and exclusion criteria, and the study was approved by the Research Ethics Committee of the Institute of Molecular Biology and Biotechnology, Bahauddin Zakariya University, Multan, with notification No. IMBB/02/2021.

2.2. Inclusion and exclusion criteria

A number of 200 individuals were included in this study dataset. The Pakistani patients were assessed through a retroactive analysis of medical records from a collaborating institute. The included variables in this study were demographic, clinical, and biochemical markers related to the risk assessment of cancer. Each individual was assigned a unique patient ID that served as a unique identifier. Age (recorded in years ≥18) and Gender (categorized as Male or Female) provided essential demographic information. During patient interviews, lifestyle factors like smoking (Yes/No) and alcohol intake (Yes/No), as well as family history of cancer (Family_History, binary: Yes/No) were self-reported. Clinical biomarkers included hemoglobin levels (g/dL), WBC_Count (white blood cell count, ×10/L), liver function tests (ALT and AST, enzymes suggesting hepatic damage), and AFP_Level (alpha-fetoprotein, a tumor marker). Clinically validated by histological or imaging confirmation, the goal variable, Cancer_Risk, was a binary outcome (0 = Low risk, 1 = High risk). Consistency was guaranteed by data preparation, which used mode imputation for categorical variables and median imputation for numerical variables to fill in missing values. Prior to data collection, ethical approval and patient consent were acquired, guaranteeing adherence to institutional review board procedures [17]. Similarly, the healthy individuals with no previous family history of cancer were included as controls and signed the consent form. The cases with multiple types of cancers, previous family history of cardiovascular diseases, and non-agreed cases were excluded.

2.3. Data mining

The genes were selected based on their strong connection with HNC and 5% allele frequency [16]. Data mining is critical in medico-biological and biomedical research investigations for extracting relevant and important informational facts [18]. This evaluation study was performed to find important genes. All genes collected from various datasets and databanks were curated and altered using the DAVID program to obtain their gene symbol, name, and UniProt IDs. To assess the functional role and annotation of selected genes, the CTD (Comparative Toxicogenomic Database), OMIM (Online Mendelian Inheritance in Man), MeSH, and PubMed databases were used [19].

2.4. Mutation analysis

The human genome has several single-nucleotide variations (SNVs). Single-nucleotide mutations cause almost 21% of amino acid changes at various protein locations (post-translational modifications), which handle pathogenesis, including cancer. Chemical changes to amino acids can influence the activity of proteins. The Active Driver, an online database, was utilized to analyze and assess alterations in genes relevant to HNC. We examined the needle plot, which provides a visual assessment of the site of mutation, frequency of mutation, and functionality of all changes detected in our genes. Protein sequences were analyzed for possible disordered regions, as well as posttranslational modification (PTM). The report illustrates the impact of related mutations and alterations, while the visualization evaluates pin location with gene and protein sequences. It offers a graphic representation of every gene alteration's location, frequency, and function.

2.5. Gene ontology and pathway enrichment analysis

Gene Ontology (GO) was analyzed to express the important signaling for the biomolecular activities of selected genes and their cellular mechanisms to investigate the biomolecular processes responsible for the upregulation or downregulation of obtained expressed genes. The KEGG pathway and the DAVID tools were used to study enriched pathways and genetic annotation [20]. To identify the significant GO terms of all DEGs, the false discovery rate (FDR) as a cut-off parameter of genes was set at <0.05, p-value ≤ 0.05.

2.6. Protein-protein interaction analysis

Protein-protein interactions (PPIs) are important to overview the biological networks [21]. PPI shows that each protein interacts with one or more proteins, either directly or indirectly, that are linked to molecular activities. It creates biological networks that depict changed activity in either normal or pathological situations. In our analysis, the top-ranked HNC-related genes' protein–protein interactions (PPIs) were examined using the STRING database version 11.0, and a network of interactions was constructed to highlight the important gene signatures functionally connected with the HNC [22]. The protein network was built using neighborhood scoring with a high confidence score (> 0.99) [23]. The annotated keywords (<0.05) were observed in this study.

2.7. Co-expression analysis

Co-expression analysis helps to understand the co-regulation and co-expression of genes. This analysis reveals the interactions of source proteins with other molecular functions, showing expression patterns. In this pattern, the networks are versatile for inquisitive diseases and correlate at the transcript level. The STRING database was used to study the co-expression of *SULF1, OAS3,* and *IFNG* genes. Co-expression showed (confidence score > 0.99) the significant genes and their signatures directly or indirectly interrelating to the target genes.

2.8. Toxicogenomic analysis

Toxicogenomics is the use of genetic data to forecast the effects of toxicants on specific genomic transcriptions, which aids in the medication development process. A comparative toxicogenomic database (CTD) was utilized to conduct a toxicogenomic study to investigate the interaction of toxicants with target genes. These data were used to examine genome-to-chemical-to-phenome correlations to deduce the functioning of biological pathways and signaling mechanisms that contribute to illness development and are regulated by environmental exposures. This allows for a better grasp of information relating to gene-protein chemical and illness connections, which exposes specific gene activity or expression-related gene-disease associations [24].

2.9. RNA extraction and quantification

A 200 μl sample of blood was taken in a microfuge tube, and 100 μl of lysis buffer was added to it. Initially, it was vortexed for 15 s and chilled on ice for 10 min (vortexed twice in a 10-min incubation). Then, it was centrifuged at 4500 rpm for 1 min, and the supernatant was wasted without disturbing the pellets. We resuspended the pellet in 600 μl lysis buffer, vortexed it again, and centrifuged it at 4500 rpm for 1 min. The supernatant was discarded, and this process was repeated until we got a white pellet. One ml triazole was added to it and dissolved by pipetting. These pellets were incubated for 10 min at room temperature, followed by the addition and mixing of 200 μl chloroform. This mixture was incubated again for 2–5 min at room temperature and later on, centrifuged at 12000 rpm for 15–17 min at 4°C. An upper aqueous layer was shifted to a pre-chilled new tube. Isopropanol was added in an equal ratio, and tubes were incubated on ice for 10 min. It was centrifuged at 4°C and 12000 rpm for 10 min. The supernatant was cast off, and the pellets were washed with 100 μl of 75% ethanol. It was centrifuged at 7500 rpm for 5 min at 4°C, followed by air drying and dissolution of the pellet in 40 μl of RNA-free water, and finally, the extracted RNA was stored at −80°C with the help of RNA stabilizer. Later on, quantification of RNA was made at 260, 280, and 320 nm using a Nanodrop (model: Skanit RE 4.1, Thermo Scientific, Waltham, MA, USA).

2.10. cDNA synthesis

Using a cDNA synthesis kit (Vivantis cDSK01-050), the RNA was used to synthesize cDNA according to standard guidelines. The RNA primer genes were combined with 10 μl of the previously produced mix of cDNA synthesis. After centrifugation at 12000 rpm for 60 min, RNA samples were placed in an incubator at 40°C. To stop the process, the tubes containing the mixture were then incubated for five minutes at 85°C. Finally, the tubes were placed on ice to chill them for about 5 min before being centrifuged under the same circumstances. The cDNA was synthesized and immediately utilized for further investigation.

2.11. Quantitative Real-Time PCR (qRT-PCR) analysis

RNA quantification offers the level of cDNA synthesis. At the wavelength of 260:280, ratios between 1.5 and 2.7 show good-quality RNA with 800–1250 ng/ml quantity. Using the relative $2^{-\Delta\Delta CT}$ approach, the gene expression patterns of the HNC-related genes *SULF1, IFNG*, and *OAS3* were examined and evaluated. Through absolute quantification, a C_T (threshold cycle) value was obtained, signifying the quality and the authentic significance of its manifestation. An online server, Primer Bank, was used to design the HNC-related primers of the HNC-related genes. The cDNA was synthesized and was directly used for further investigations [25]. For validation of HNC-related genes, qPCR was completed using MIC-PCR (Bio Molecular Systems, Australia) under standard conditions. An ultimate 20 μl volume of the reaction mixture was made using 4 μl of cDNA (1:10), 5 μl of the SYBR Green master mix, and 0.5 μl of each gene-specific forward and reverse primer. This volume was confirmed with RNAs free of water, and the reaction mixture's conformation remained constant for both the genes and the reference genes. The expressions of the reference and examination genes were measured using a two-step qPCR process, with the GAPDH gene serving as a housekeeping or internal reference gene. The comparative level of expression of each gene was computed with reference to *GAPDH* as keeping the standard value "1." The standard cycling conditions for qPCR were denaturation at 95°C for 15 min, 40 cycles of 95°C for 15 s, 57°C for 20 s, and 72°C for 20 s. The basic extension was performed for 10 min at 72°C. To determine the compensatory properties of double-stranded DNA during heating and to observe the intensity of absorbance, the qPCR results were examined using the melting curve graph. The median (average) C_T values were determined for the internal reference gene and the genes linked to HNC. C_T is the log value converted to a relative quantity. The relative $2_T^{-\Delta\Delta C}$ method was used to compute and evaluate the comparative expressions of the HNC-related genes after ΔC_T (delta threshold) for the genes being studied using the internal reference gene. The ΔC_T of the targeted gene and reference gene *(GAPDH)* was calculated. The $\Delta\Delta C_T$ (delta–delta threshold value) specifies the difference between the expression level of the HNC-related genes and the internal reference gene. Finally, $2_T^{-\Delta\Delta C}$ was evaluated, representing the fold difference of the expression of targeted genes from the control. We calculated the total association of these genes to express the comprehensive expression levels. The hierarchical cluster of genes showed the expression pattern using the online one-matrix CIMminer tool [26].

2.12. Statistical analysis

SAM software was used to conduct the statistical analysis, and the results were presented as standard errors and standard deviations.

3. Results

3.1. Data mining and selection of genes

The text mining helped curate significantly associated HNC genes. For functional annotation, cross-verifications, and shortlisting of these genes, we used the DAVID tools, Comparative Toxicogenomic Database (CTD), OMIM (Online Mendelian Inheritance in Man), MeSH, and PubMed databases [19]. Candidate genes were selected based on >5% allele frequency and significant association of genes with HNC ($p < 0.05$) (Fig. 1).

3.2. Mutation analysis

This analysis suggests that these mutations might interfere with methylation activities, which are crucial for controlling the connections and functions of proteins. *IFNG* had four post-translational modification (PTM) spots with 33 frequent transformations at the negative strand of chromosome 12, coding 166 protein deposits, showing 9.04% of the expected disordered region. The visualization of the mutation plot exhibited *IFNG* isoforms' direct mutation influences between 48 and 120 with reference amino acid (AA) residues N (ASN) on both sites and mutated amino acid residues K (LYS) and T (THR), respectively. Motif-changing mutation impact on 122 with reference AA residue S (SER) and mutated AA residue (LEU), proximal mutation impact on 75 with

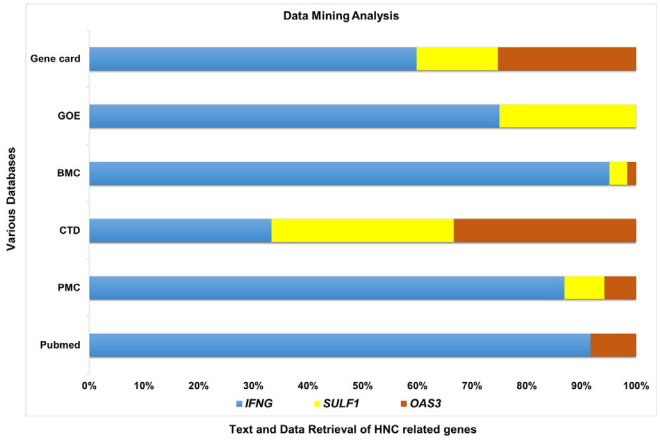

Fig. 1. Data mining and cross-analysis of HNC-related genes using different databases.

reference AA residue F (PHE) and mutated AA residue L (LEU), and similarly distal mutations impact on 44, 86, 88, 115, and 126 with reference AA residue D (ASP), S (SER), F (PHE), and L (LEU) and mutated AA residue Y (TYR), N (ASN), I (ILE), and F (PHE), respectively. The mutation site of *IFNG* at position N48S confined 'N' amino acid residues enriched with an N-glycosylation, glycosylation, and phosphorylation direct mutation impact. *IFNG* N120T contained N residues with N-glycosylation, glycosylation, and N-glycosylation; glycosylation motif-changing mutation affects a protein's 120 position. The *IFNG* mutation at location F75L resulted in restricted S amino acid deposits that were amplified by a phosphorylation-proximal mutation effect. Phosphorylation-distal mutation imprints were observed as S clusters (serine residues) in the D86Y variant, spanning 92 protein sites. However, *OAS3* showed 2.39% of the expected confused area on the positive strand of chromosome 12 with 26 PTM sites and 205 recurrent mutations coding 1087 protein deposits. The mutation plot visualization showed the proximal mutation effects of OAS3 isoforms between 373 and 451, 460, and 1691 sites with reference amino acid (AA) remainders N (ASN), H (HIS), G (GLY), and L (LEU) and mutated amino acid remainders K (LYS), Y (TYR), V (VAL), and I (ILE), respectively. Distal mutation impression on 461, 464, 802, 814, and 966 with reference AA residue S (SER), R, G, R, and L and mutated AA L (LEU), Q (GLN), D (ASP), H. The mutation site of OAS3 at position S461L confined the S amino acid cluster enriched with a phosphorylation and K residue with ubiquitination distal mutation impact (Fig. 2) and I (ILE), respectively. The mutation site of *OAS3* at location L691I confined K amino acid deposits supplemented with sumoylation proximal mutation impression. *OAS3* N373K confined S deposits with phosphorylation and K with ubiquitination mutation impressions at the 369 and 370 locations of the protein. The mutation site of *OAS3* at position S461L confined the S amino acid cluster enriched with a phosphorylation and a K residue with ubiquitination distal mutation impact (Fig. 2).

3.3. Gene ontology and pathway enrichment analysis

GO and KEGG pathway enrichment analyses were carried out using DAVID to examine the biological classification of genes. Changes in genes' biological processes were primarily "enriched" according to GO analysis results.

The gene ontology of HNC-related genes presented significantly improved terms. We annotated HNC-related genes with known cellular components, biological processes, and molecular functions. It was observed that HNC-related genes remained tangled in other biological processes like responses in immunity against the virus, production of encouraging regulation factor of tumor necrosis, defense response to the virus, and apoptotic processes. Their cellular components were found in the extracellular space. Cytokine was associated with the molecular functions of genes having ligase, hydrolase, catalytic, and transcriptional activities. The role of the selected genes in biological pathways was predicted in DNA replication, immune response, energy metabolism, and regulation of nucleotides. The pathway enrichment showed their role in interferon gamma signaling, pyrimidine biosynthesis, initiation and termination of RNA polymerase I transcription, formation of early elongation complex, RNA polymerase II, and nucleotide excision repair pathways (Fig. 3). In enrichment analysis, it was observed that HNC genes are linked with other functional pathways, including hepatitis, influenza A, and herpes simplex virus pathological pathways; metabolic and catabolic processes; mRNA processing; signal transduction; intracellular transport; protein transport; and other essential biological activities that are all directly and indirectly related to *SULF1, IFNG*, and *OAS3* ($p < 0.05$).

3.4. Protein-protein interaction network analysis

A complex interaction network with multiple interaction patterns was produced by the STRING evaluation of all the aforementioned genes.

It was predicted that these molecules have direct or indirect functional associations. The PPI network confined nodes (each node indicates specific proteins) and the edges. The network displayed the genes having enriched co-expression (PPI enrichment, $p < 1.0$) and functional association with different genes. *OAS3* has a direct association with *ADAR,* which is an adenosine deaminase specific to double-stranded RNA that catalyzes the hydrolytic conversion of adenosine to inosine in dsRNA, also known as RNA editing. Changing the codon sequence can disrupt gene expression and functions in several ways, including mRNA translation. Therefore, the sequence of amino acids is changed, and consequently, the functional proteins are dysregulated. *DDX5* is a receptor that has an antiviral innate immune response and senses cytoplasmic nucleic acids of the virus. It activates a downstream signaling cascade, producing type I interferons. With viral RNAs, it forms a ribonucleoprotein complex. *SP100,* which is a nuclear autoantigen. In collaboration with PML, which is a tumor suppressor and is a major fundamental of the PML bodies, it is a subnuclear organelle involved in several biological processes, such as cell proliferation, cell differentiation, and apoptosis. In some circumstances, it functions as a coactivator in the transcription of *ETS1* and E*TS2*. Guanylate-binding protein-1 has antiviral activity against the influenza virus and hydrolyzes GTP to GMP in two consecutive cleavage events. It provides a wide range of host protection against several pathogenic groups by bringing antimicrobial peptides to autophagolysosomes and encouraging oxidative death. *OAS3, PIGR, STAT2, HLAE, ROHA*, and *CXCR4* are directly associated with IFNG, while EGRF is an epidermal growth factor receptor. It is an *EGF* family receptor of tyrosine kinase-binding ligands that initiates many signaling channels to convert extracellular signals into appropriate cellular responses. *IL1B,* interleukin-1 beta, is a strong pro-inflammatory cytokine. It is involved in the activation of T-cells and cytokine production, activation of B-cells, production of antibodies, production of collagen, and proliferation of fibroblasts. It promotes T-cell differentiation and induces the synthesis of *IFNG* from T-helper 1 (Th1) cells. *IRF5* is an interferon regulatory factor-5 and a transcription factor that contributes to the activation of IFNA and *IFNB* interferons and inflammatory cytokines in response to viral infection. It belongs to the *IRF* gene family that contributes to head and neck cancer. *SULF1* has a functional association with *POSTN* and periostin and induces cell attachment and adhesion of

Fig. 2. Analysis of mutation of HNC-related genes representing post-translational modifications with significant cut-off values. It represents the important sites of the protein that are disordered and contribute to a pathophysiological role and development of the disease.

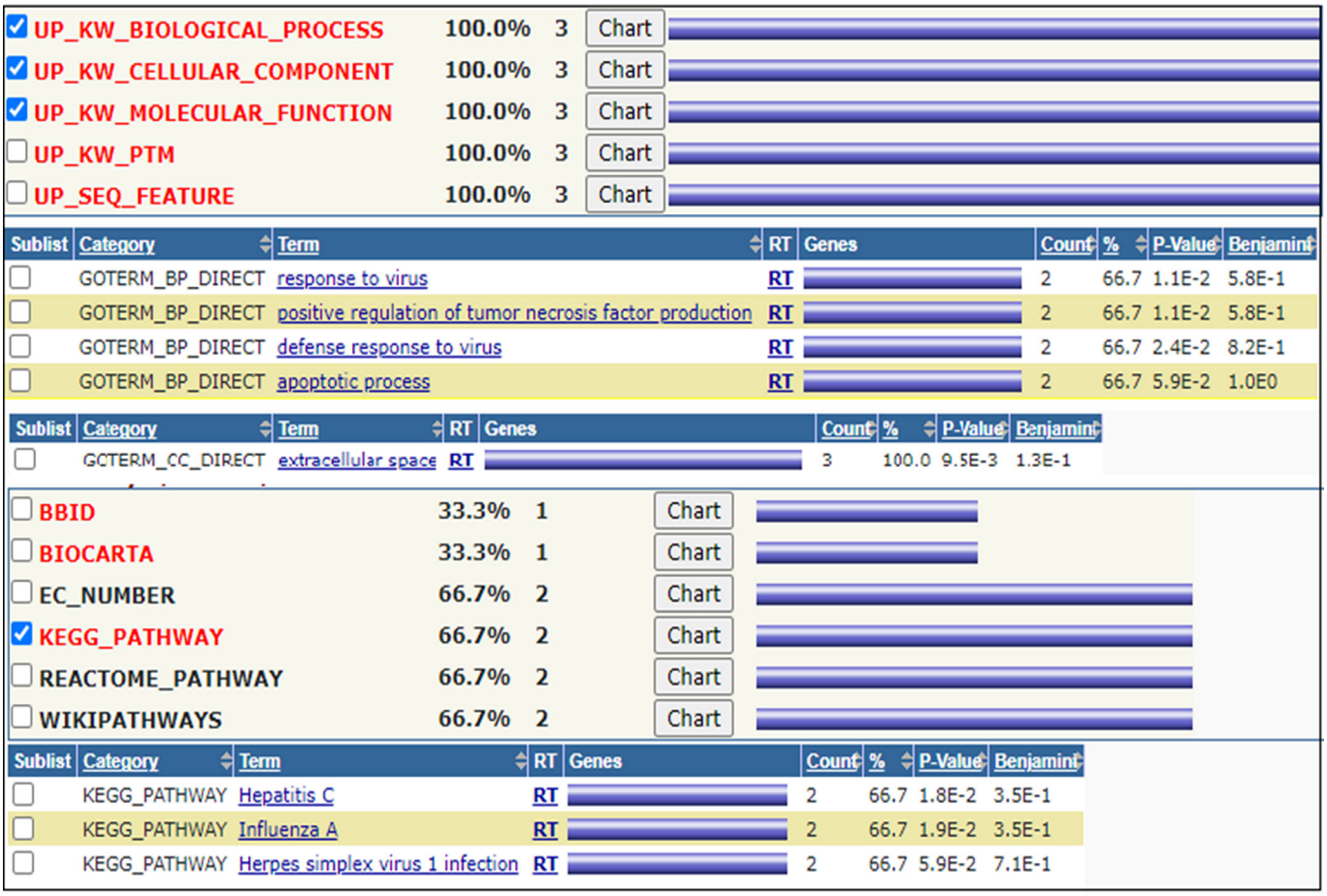

Fig. 3. Gene Ontology and enrichment analysis using DAVID tools.

the cell. It increases *BMP1* integration in the fibronectin matrix of connective tissues and consequently activates lysyl oxidase *LOX* proteolytically. *SCEL,* sciellin, functions in the protein's assembly in the cornified envelope. *SYNPO*, or synaptopodin, is a protein that is actin-associated and alters the movement and structure of spines and renal podocyte foot procedures dependent on actin. It seems to be crucial for the development of spinal apparatuses, which are involved in synaptic plasticity, and *EXT2*, Exostosin-2, glycosyltransferase is mandatory for the heparan-sulfate biosynthesis. The *EXT2* is a tumor suppressor and is compulsory for the exosomal release of *SDCBP, CD63,* and syndecan. It is well recognized that certain genes, such as HRAS, CCND1, and CDKN2A, are responsible for cell cycle progression and apoptosis, linked to cancer. This implies that mutations in these genes may interfere with its interactions with the hub genes, which may result in unregulated cell proliferation, indicative of cancer.

These variations in these functional interactions may lead to the development of head and neck cancer (Fig. 4).

3.5. Co-expression analysis

The genes were used to further investigate their expression and their correlation pattern in order to confirm our findings.

IFNG is associated with macrophage activation and has antiproliferative and immunoregulation functions. This gene is associated with *IFNGR2* for binding a receptor of the induction of interferon. This ligand binding activates the JAK/STAT signaling pathway and has a significant function in the IFN-gamma pathway. This pathway is important for cellular responses to infectious agents. Similarly, interleukin-1 beta is an inflammatory cytokine, and it induces prostaglandin synthesis, activation of T-cells, neutrophil influx, production of cytokine and antibody, and proliferation of fibroblasts.

SULF1 has arylsulfatase activity, which is highly specific endoglucosamine-6-sulfatase activity. It binds to *SLCO5A1* and belongs to the 5A1 family of organic anion transporters and is a solute carrier. It is involved in the assembly and regulation of proteins. It also plays a part in other biological functions, such as gene regulation, cell proliferation, differentiation, and cell death. It synthesizes a 2′-5′-oligoadenylates dimer from ATP, which formerly binds to the inactive ribonuclease that leads to its dimerization and subsequently its activation. The activation of RNase degrades the cellular as well as viral RNA (Fig. 5).

3.6. Toxicogenomic analysis

The CTD provides information about chemicals, chemical phenotypes, gene ontology, and chemical-disease associations. The search for genes related to HNC was based on the CAS number of each individual carcinogenic and inference network.

In this network, HNC-associated expressed genes were investigated for their activity and expression associated with different environmental chemicals. The activity and expression of these genes are increased or decreased. This variable expression of gene activity at different cellular events can affect the co-treatment expression of different genes, leading to the incidence of the disease. It was discovered that different genes with the same chemical exposure may show different reactivity. We observed that targeted genes could respond and be transcribed differently to various toxicants. We found that silicon dioxide, valproic acid, and bisphenol

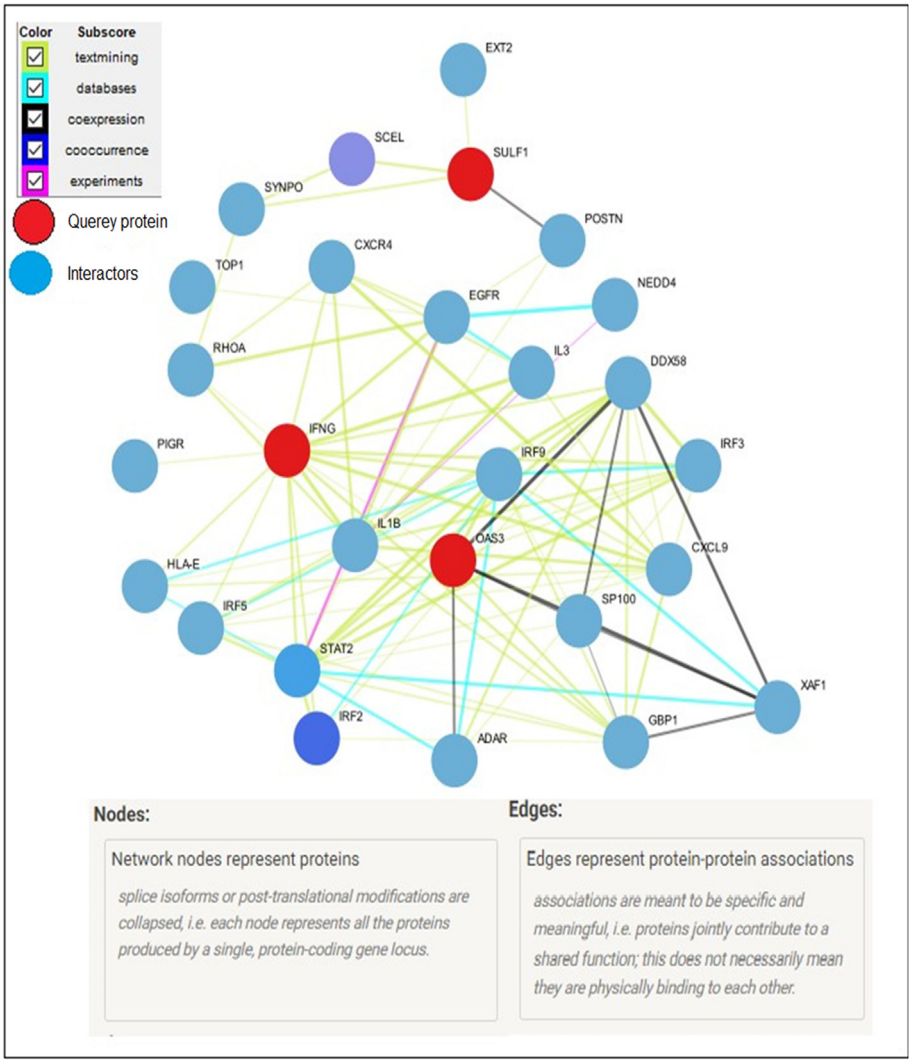

Fig. 4. Protein-protein network interaction indicates the interaction of source proteins with target proteins. Each node represents the protein, and edges show the interactions.

are highly toxic and dysregulate the *SULF1* expression. Similarly, nitric oxide has a high level of toxicity to *IFNG* and *OAS3* expression patterns. *OAS3* expression profile is more susceptible to lipopolysaccharide, while tetrachlorobenzodioxin is a common toxicant to *IFNG, OAS3*, and *SULF1*. We studied that some drugs, including reversitol, inomysin, picric acid, cisplatin, cyclosporin, cadmium chloride, atrazine, and aflatoxin, are moderately toxic (Fig. 6).

3.7. RT-qPCR analysis and expression profiling

The RT-qPCR is reliable in limiting the resulting product from exhibiting a higher fluorescence signal. We performed expression profiling to identify the changes happening in the expression of genes that are correlated with HNC. We extracted the total RNA of selected genes by triazole extraction of serial dilutions from fresh blood and analyzed the expression profiles of genes in duplicates among cases and controls. To classify targeted genes that showed differential expression among the healthy and cases in a significant method, we used the SAM software, which calculates false discovery rates (FDRs) and a threshold (Δ) for statistical significance and fold-change. By using a highly substantial threshold of a median, estimated at less than 1%. Two-dimensional hierarchical clustering using the CIMminor tool was performed to study the expression profiles among samples. The relative expression showed that *SULF1* is downregulated, while *OAS3* and *IFNG* are upregulated at two-fold change levels (2_{T}^{-DDC}) that were significant compared to controls. These expressed genes were irrationally expressed and are involved in disease development and progression. In our analysis, we studied and quantified the expression profiles of these genes among cases and controls. We observed significant changes and aberrant expression in cases compared to controls. In Fig. 7, we identified that *IFNG* and *OAS3* have differential expression and are substantially overregulated compared to control, while *SULF1* is downregulated. Cluster analysis was used to examine the gene expression patterns of the two categories (the control group and patients) that had noticeable expression patterns. The expression of samples is shown in the image as columns, and the genes with different expression patterns are shown as rows (Fig. 8). We observed that the maximum number of the samples of *IFNG, SULF1*, and *OAS3* genes showed differential expression patterns compared to the controls. These genes that are expressed either contribute to the same physiological role or have a related biological function. Genes with increased expression levels were grouped into clusters, and in many samples, we identified significant clusters characterized by distinct expression patterns (fold change ≥ 2 and $p < 0.05$).

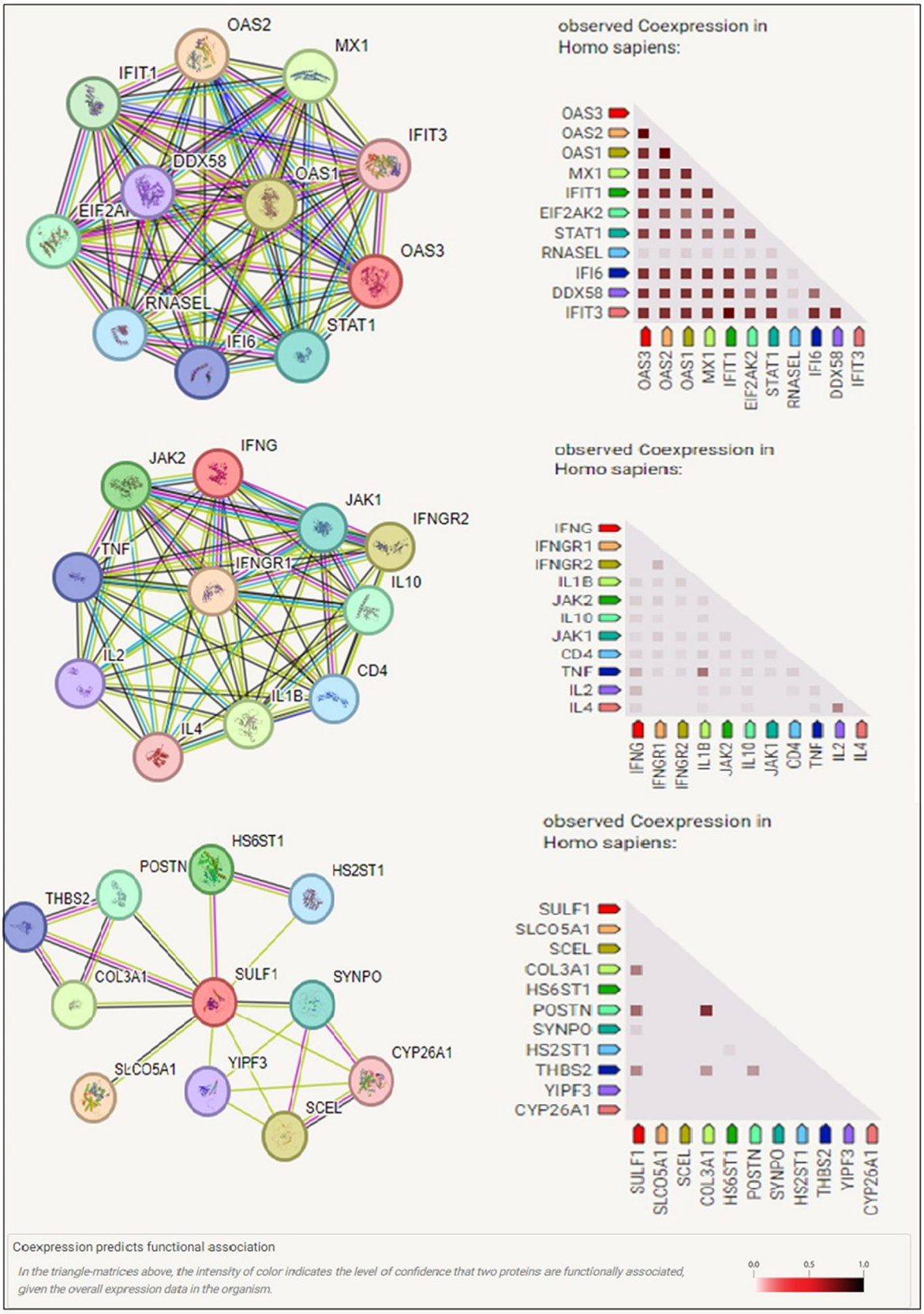

Fig. 5. The STRING database generated a co-expression network of proteins based on the neighborhood scoring with a > 0.99 confidence score. Proteins are represented by nodes and interactions by edges.

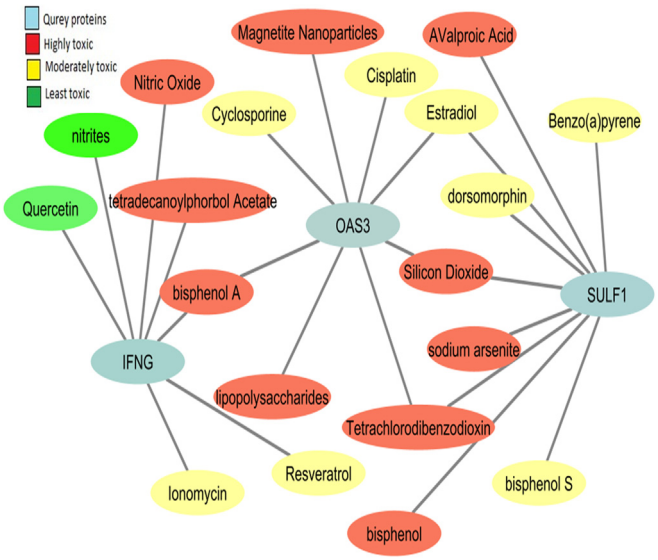

Fig. 6. Toxicogenomic analysis shows the interactions of various toxicants with HNC-related genes, presenting how such chemicals would affect the genetic transcription.

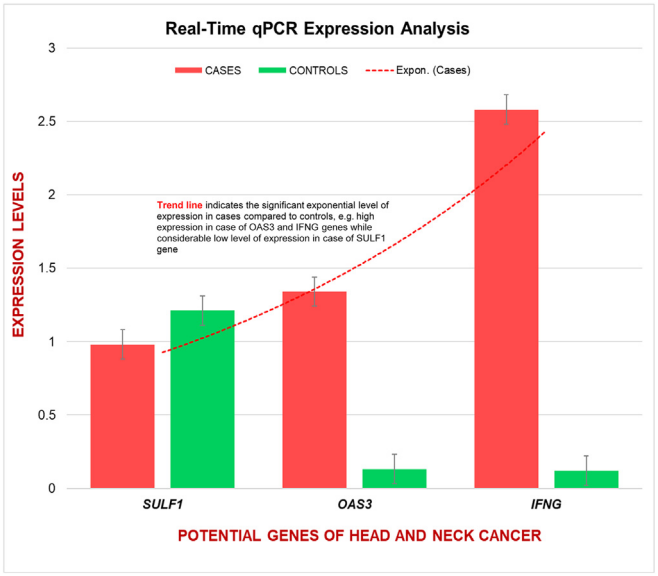

Fig. 7. Quantitative real-time PCR shows the normal and aberrant expression levels of HNC-related genes among diseased and control on the fold change base of gene expression.

4. Discussion

Patients' lives and health are seriously threatened by head and neck cancer. Although the exact cause of stomach cancer is still unknown, a number of factors, such as nutrition, lifestyle, environmental factors, and genetic susceptibility, are thought to have a role. HNC frequently has non-specific early clinical signs. Most patients are dependent on conservative therapy by the time their symptoms become severe. Although the evaluation criteria for solid tumors are commonly used to evaluate the effectiveness of anticancer medications, they may not accurately predict prognosis. Therefore, improved efficacy evaluation and prognosis prediction require the identification of more trustworthy tumor markers to better measure tumor existence and growth [27]. Bioinformatics has undergone a revolution thanks to machine learning, a potent artificial intelligence technology that makes it possible to create complex models that can analyze large datasets and reveal complex patterns. Numerous review research publications have addressed the use of bioinformatics in the detection of various cancers, including lung, breast, liver, oral, brain, and ovarian [5,6]. Numerous sectors and fields of study have changed as a result of the quick development of algorithms, computing power, and data volume and velocity. By leveraging the data gathered to make these adjustments and better adapt to their new customer demands, this can help firms get ready for these changes. Automotive, banking, healthcare, and manufacturing are just a few of the industries that can greatly benefit from improved and expedited data synthesis [7]. Deep learning has emerged as one of the most important and effective machine learning techniques in recent years. This has improved the state-of-the-art performance of numerous machine learning tasks and enabled the advancement of numerous disciplines [28]. This study investigates the expression and functional enrichment of genes associated with head and neck cancer. We found *OAS3, SULF1*, and *IFNG* are identified as potential biological targets or biomarkers of HNC through bioinformatics analyses and real-time expression studies. Differential expression of these genes was examined between healthy and diseased individuals; expression profiling showed obvious differences between the two groups. Some genes were upregulated while others were downregulated. The dysregulated expression of these genes affected various physiological activities, including cancer pathways such as immune response, DNA repair mechanism, oxidation, metabolism, and signaling. Our analysis also identified some interacting genes, such as SP100 and STAT6, as possible therapeutic drug targets that interact with our genes [29]. These genes encode drug-metabolizing enzymes that carry chemically induced inherent mutations and play an important role in cell differentiation and growth [30,31]. Analysis of human proteomic data is based on post-translational modifications (PTMs), which are important regulators of protein functions and signaling pathways; therefore, they help interpret deleterious missense mutations by analyzing inter-individual genetic variations [32]. The studied genes are reported to contribute to various types of cancers or cancer-associated pathways in the literature. Interferon-gamma (*IFNG)* is a precursor gene that encodes a soluble cytokine that belongs to the type II interferon class. These innate and adaptive immune cells of immune system secrete this encoded protein. This is a homodimer of a dynamic protein that ligates to the interferon-gamma receptors that trigger cellular defenses against microbial and infectious diseases. If this gene is mutated, it will have an amplified vulnerability to viral, parasitic, and bacterial infections and several autoimmune diseases [33]. The *IFNG* protein has a high association with an elevated risk of tumors in the breast, lungs, stomach adenocarcinoma, head and neck carcinoma, and many other types. It was reported previously that there is a significant correlation between *SULF1* and *BRCA,* as high *SULF1* expression in tissues may promote tumor growth and metastasis. Some researchers have proposed that inhibiting *SULF1* may target tumor cells by down-regulating the RTK pathway [34]. Increased levels of secretion of *SULF1* enhance the modification of the extracellular matrix in the tumor environment, resulting in the development of tumors in the adjacent host cells [35]. Similarly, *OAS3* is 2-5-oligoadenylate synthase 3 gene that encodes for an enzyme incorporated in the 2,5-oligoadenylate synthase family. The interferons induce this enzyme, and it catalyzes the 2,5 oligomers of adenosine for binding and stimulation of RNase L. This enzyme family plays a substantial role in inhibiting cellular protein synthesis and resistance against viral infections [34]. The *OAS3* enzyme is majorly associated with a great risk of tumors in the rectum, liver, lungs, head and neck carcinoma, and many other types [36,37]. The

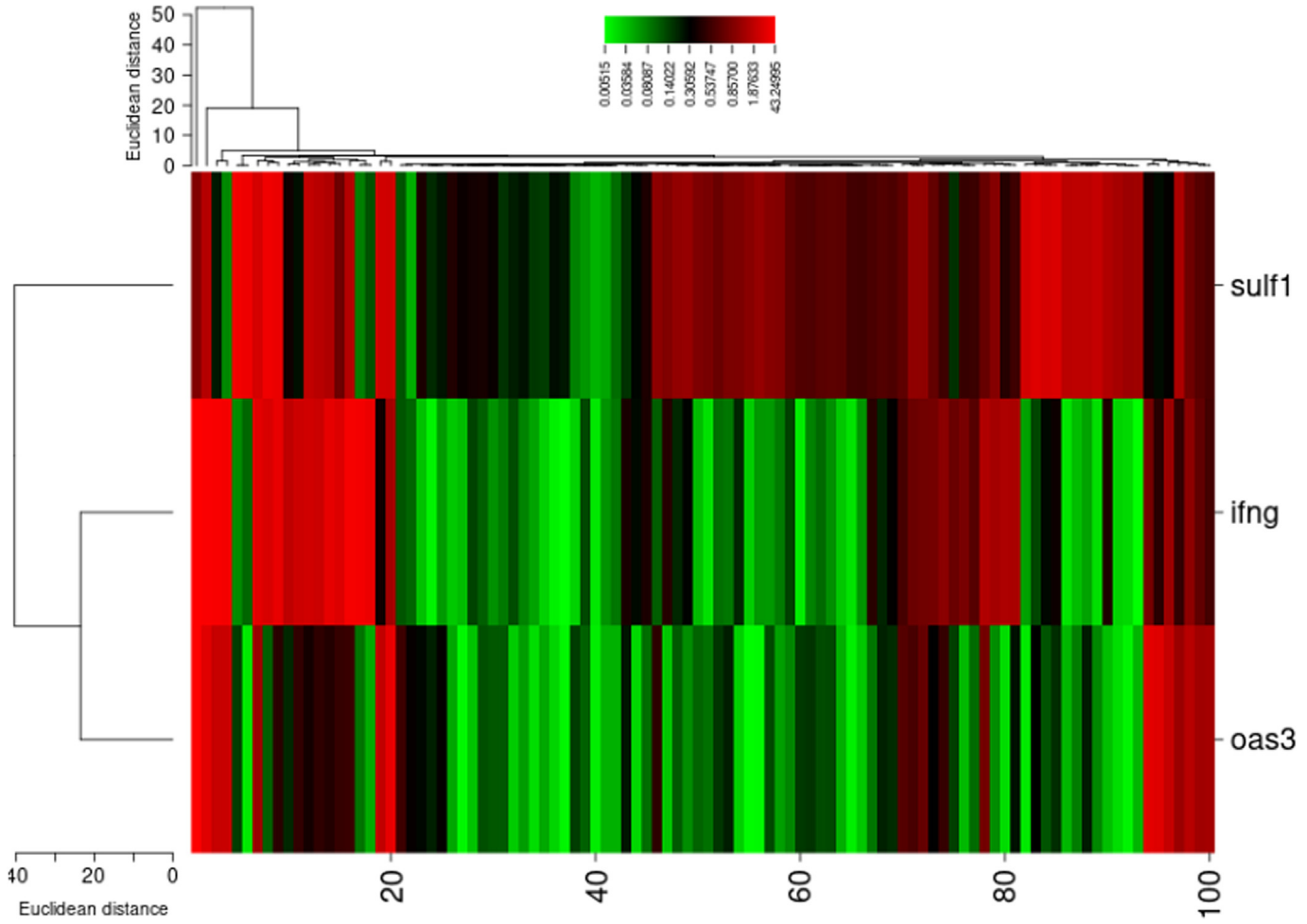

Fig. 8. Heat map of hierarchical cluster analysis representing the expression profiles of differentially expressed genes (*IFNG, OAS3,* and *SULF1*). The columns represent the sample numbers, and the rows represent the differentially expressed genes.

OAS3 expression was positively interrelated with 47 genes that are immune checkpoints in most cancer types [38].

In recent studies, protein networks help to curate the functional proteins and hub genes in identifying biomarkers involved in tumorigenesis, prognosis, and drug resistance [39,40]. The PPI network plays a vital role in the association of these genes with disease. The predicted associated gene may have a pivotal role in the metabolism of xenobiotics, progression of tumors, cell cycle suppression, alcoholism, and microRNA signaling pathway [41]. Integrating protein into a human protein–protein interaction network discovered important aspects of hubs and cancer-related proteins. It is difficult to find the comparative position of a specific protein in an extremely complicated PPI network. To measure the comparative location of specific proteins in the complex network, we computed the connectivity distance between the nodes. This information connects a protein with other important proteins. This expressed the strong interrelation with one another, representing a general agreement between different proteins. We obtained three HNC genes by constructing a PPI network comprising *PIGR, HLAE, IRF5, STAT2, IL1B, IRF9, IRF3, SP100, GBP1, ADAR, XAF1, CXCL9, POSTN, SYNPO,* and many others. Most of them are associated with tumorigenesis and the progression of cancer patients, such as *POSTN* [42], *PIGR* [43], *IRF3*, *ADAR* [44], and *STAT2* [45].

The results of gene ontology showed that these genes were involved in similar biological processes. In these annotations, *IFNG, SULF1,* and *OAS3* were mainly enriched in biological processes that prevent viral genome replication and regulate the immune system and apoptotic and necrosis regulation pathways. Proteins encoded by *OAS* family genes activate RNase, which degrades viral mRNA and inhibits viral protein synthesis [46,47,48,49]. We observed that high expression of the *OAS* gene family as a defense strategy in response to virus infection may then induce cell proliferation, which leads to the HNC development. Diagnostic strategies are getting attention for analyzing the effect of different toxicants in cancer risk assessments [50]. Recent advancements in toxicogenomic analyses have facilitated new opportunities for the assessment of cancer risk. Incorporating the interaction of chemical gene has exposed different environmental chemical exposures to the development of disease. The toxicogenomic analysis facilitates revealing the mechanism between the chemical and the related gene products and the effect of this interaction on human diseases that are influenced by environmental exposure [51,52].

RT-qPCR is gaining worth at the molecular level for genetic assessments, and by using this technique, we quantitatively evaluated the expression profile of these genes (*IFNG, SULF1,* and *OAS3*). We found that two genes, *IFNG* and *OAS3,* were overexpressed and *SULF1* was downregulated. Some studies showed that *IFNG* is down-regulated in HNC and other cancers. It has been validated in the previous investigations that *TNF-*α and *IFN-*γ are downregulated compared to controls [53,54]. *SULF1* is downregulated with HNC, and similarly in other studies, the parallel pattern of expressions is observed [55,56]. A study showed that *SULF1* is involved in the proliferation's inhibition and invasion of esophageal squamous

cell carcinoma (HNC) via regulation of the heparin-binding growth factor signaling pathways [57]. Many diseases, including autoimmune disorders [58], HNC, other cancers [59], viral diseases [60,61], and persistent infections, are linked to the *OAS* gene family.

5. Conclusions

Our integrative framework showed potential therapeutic targets of cancer that could reveal genotype-to-phenotype associations. We found a significant correlation between *SULF1, OAS3,* and *IFNG* genes with HNC. RT-qPCR analysis and expression profiling of these genes provide system-level analysis showing the pathological role of these genes. These genes could be potential biological targets or biomarkers and can be helpful in upgrading therapeutic strategies.

CRediT authorship contribution statement

Juweria Khawar: Writing – original draft, Methodology, Investigation. **Jinlei Guo:** Writing – original draft, Investigation, Formal analysis. **Saeed Akhtar:** Writing – review & editing, Investigation, Formal analysis. **Baogang Bai:** Writing – review & editing, Methodology, Formal analysis. **Syed Aun Muhammad:** Writing – review & editing, Supervision, Methodology, Investigation, Conceptualization.

Financial support

This research did not receive any specific grant from funding agencies in the public, commercial, or not-for-profit sectors.

Declaration of competing interest

There is no conflict of interest among authors. The authors declare that the research was carried out in the absence of any commercial or financial relationships that could be understood as a potential conflict of interest.

Acknowledgments

We are thankful to all lab members of the Biopharmaceutical Informatics and Systems Biology Lab of the Institute of Molecular Biology and Biotechnology, BZ University Multan, for their support and encouragement while carrying out my research work.

Supplementary material

https://doi.org/10.1016/j.ejbt.2026.100705.

Data availability

No data was used for the research described in the article.

References

[1] Addala L, Pentapati CK, Thavanati PR, et al. Risk factor profiles of head and neck cancer patients of Andhra Pradesh, India. Indian J Cancer 2012;49(2):215–9. https://doi.org/10.4103/0019-509X.102865. PMid: 23107973.
[2] Mody MD, Rocco JW, Yom SS, et al. Head and neck cancer. Lancet 2021;398 (10318):2289–99. https://doi.org/10.1016/S0140-6736(21)01550-6. PMid: 34562395.
[3] Rahman QB, Iocca O, Kufta K, et al. Global burden of head and neck cancer. Oral Maxillofac Surg Clin North Am 2020;32(3):367–75. https://doi.org/10.1016/j.coms.2020.04.002. PMid: 32482563.
[4] Datorre JG, Dos Reis MB, Sorroche BP, et al. Intratumoral *Fusobacterium nucleatum* is associated with better cancer-specific survival in head and neck cancer patients. J Oral Microbiol 2025;17(1):2487644. https://doi.org/10.1080/20002297.2025.2487644. PMid: 40182114.
[5] Ahmad Z, Idress R, Fatima S, et al. Commonest cancers in Pakistan-findings and histopathological perspective from a premier surgical pathology center in Pakistan. Asian Pac J Cancer Prev 2016;17(3):1061–75. https://doi.org/10.7314/apjcp.2016.17.3.1061. PMid: 27039726.
[6] Dylawerska A, Barczak W, Wegner A, et al. Association of DNA repair genes polymorphisms and mutations with increased risk of head and neck cancer: A review. Med Oncol 2017;34(12):197. https://doi.org/10.1007/s12032-017-1057-4. PMid: 29143133.
[7] Rani P, Shivaprasad MM. Emerging insights into supari (areca nut) toxicity: A review of current evidence on oral and general health. Toxin Rev 2025;44 (3):383–96. https://doi.org/10.1080/15569543.2025.2538139.
[8] Nosé V, Lazar AJ. Update from the 5th Edition of the world health organization classification of head and neck tumors: Familial tumor syndromes. Head Neck Pathol 2022;16(1):143–57. https://doi.org/10.1007/s12105-022-01414-z. PMid: 35312981.
[9] He B, Zhu R, Yang H, et al. Assessing the impact of data preprocessing on analyzing next generation sequencing data. Front Bioeng Biotechnol 2020;8:817. https://doi.org/10.3389/fbioe.2020.00817. PMid: 32850708.
[10] Doshi R, Hiran KK, Gök M, et al. Artificial intelligence's significance in diseases with malignant tumours. Mesop J Artif Intell Healthcare 2023;2023:35–9. https://doi.org/10.58496/MJAIH/2023/007.
[11] Huang H, Huang F, Liang X, et al. Afatinib reverses EMT via inhibiting CD44-Stat3 axis to promote radiosensitivity in nasopharyngeal carcinoma. Pharmaceuticals 2022;16(1):37. https://doi.org/10.3390/ph16010037. PMid: 36678534.
[12] Pazhani J, Veeraraghavan VP, Jayaraman S. Transcription factors: A potential therapeutic target in head and neck squamous cell carcinoma. Epigenomics 2023;15(2):57–60. https://doi.org/10.2217/epi-2023-0046. PMid: 36974620.
[13] Li X, Li M, Xiang J, et al. SEPA: Signaling entropy-based algorithm to evaluate personalized pathway activation for survival analysis on pan-cancer data. Bioinformatics 2022;38(9):2536–43. https://doi.org/10.1093/bioinformatics/btac122. PMid: 35199150.
[14] Garg S, Sharma N, Bharmjeet, et al. Unraveling the intricate relationship: Influence of microbiome on the host immune system in carcinogenesis. Cancer Rep 2023;6(11):e1892. https://doi.org/10.1002/cnr2.1892. PMid: 37706437.
[15] Cai Y, Wu Q, Chen Y, et al. Predicting non-small cell lung cancer-related genes by a new network-based machine learning method. Front Oncol 2022;12:981154. https://doi.org/10.3389/fonc.2022.981154.
[16] Khawar J, Fatima N, Ismail M, et al. Studying association of *GTF2H4, SULF1, OAS3*, and *IFNG* genes polymorphism and risk of head and neck cancer in Southern Punjab, Pakistan. Meta Gene 2018;16:85–9. https://doi.org/10.1016/j.mgene.2018.02.002.
[17] Mzili T, Mzili M, Bouderba SI, et al. The role of artificial intelligence in early tumor detection: An XGBoost risk assessment model for Egyptian Patients. Mesop J Artif Intell Healthcare 2025;2025:85–92. https://doi.org/10.58496/MJAIH/2025/008.
[18] Huang C, Liu Z, Guo Y, et al. scCancerExplorer: A comprehensive database for interactively exploring single-cell multi-omics data of human pan-cancer. Nucleic Acids Res 2025;53(D1):D1526–35. https://doi.org/10.1093/nar/gkae1100. PMid: 39558175.
[19] Zheng W, Li Z, Chen Y, et al. GEP-DNN4Mol: Automatic chemical molecular design based on deep neural networks and gene expression programming. Health Inf Sci Syst 2025;13(1):31. https://doi.org/10.1007/s13755-025-00344-8. PMid: 40144479.
[20] Asim MN, Ibrahim MA, Malik MI, et al. ADH-PPI: An attention-based deep hybrid model for protein-protein interaction prediction. iScience 2022;25 (10):105169. https://doi.org/10.1016/j.isci.2022.105169. PMid: 36267921.
[21] Cui J, Yang S, Yi L, et al. Recent advances in deep learning for protein-protein interaction: A review. Biodata Min 2025;18(1):43. https://doi.org/10.1186/s13040-025-00457-6. PMid: 40524189.
[22] Singh NK, Awasthi P, Gupta A, et al. Identifying *Porphyromonas gingivalis*-infected hub genes and molecular mechanisms of oral squamous cell carcinoma pathogenesis. Discov Appl Sci 2025;7:163. https://doi.org/10.1007/s42452-024-06260-y.
[23] Zheng W, Wuyun Q, Li Y, et al. Improving deep learning protein monomer and complex structure prediction using DeepMSA2 with huge metagenomics data. Nat Methods 2024;21(2):279–89. https://doi.org/10.1038/s41592-023-02130-4. PMid: 38167654.
[24] Davis AP, Wiegers TC, Johnson RJ, et al. Comparative Toxicogenomics Database (CTD): Update 2023. Nucleic Acids Res 2023;51(D1):D1257–62. https://doi.org/10.1093/nar/gkac833. PMid: 36169237.
[25] Min D, Cheng L, Zhang F, et al. Enhancing extracellular electron transfer of *Shewanella oneidensis* MR-1 through coupling improved flavin synthesis and metal-reducing conduit for pollutant degradation. Environ Sci Technol 2017;51(9):5082–9. https://doi.org/10.1021/acs.est.6b04640. PMid: 28414427.
[26] Babicki S, Arndt D, Marcu A, et al. Heatmapper: Web-enabled heat mapping for all. Nucleic Acids Res 2016;44(W1):W147–53. https://doi.org/10.1093/nar/gkw419. PMid: 27190236.
[27] Zhang H, Jiang Y, Luo J, et al. Predictive and prognostic value of combined detection of sTim-3, PG and PD-L1 in immune checkpoint inhibitor therapy for advanced gastric cancer. Am J Transl Res 2024;16(11):6955–63. https://doi.org/10.62347/MJOA5699. PMid: 39678619.

[28] Lateef RA. Machine and deep learning techniques in cancer prediction and risk stratification using bioinformatics in big data era: A review. EDRAAK 2024;2024(11):118–27. https://doi.org/10.70470/EDRAAK/2024/015.
[29] Ivanenko K, Prassolov V, Khabusheva E. Transcription factor Sp1 in the expression of genes encoding components of Mapk, JAK/STAT, and PI3K/Akt signaling pathways. Mol Biol 2022;56(5):756–69. https://doi.org/10.1134/S0026893322050089. PMid: 36165020.
[30] Ko J, Humbert S, Bronson RT, et al. p35 and p39 are essential for cyclin-dependent kinase 5 function during neurodevelopment. J Neurosci 2001;21(17):6758–71. https://doi.org/10.1523/JNEUROSCI.21-17-06758.2001. PMid: 11517264.
[31] Hadia R, Singh V, Solanki N, et al. Unlocking the clinical significance of cytochrome P450 enzymes. Int J Pharm Investig 2024;14(1):30–8.
[32] Krassowski M, Paczkowska M, Cullion K, et al. ActiveDriverDB: Human disease mutations and genome variation in post-translational modification sites of proteins. Nucleic Acids Res 2018;46(D1):D901–10. https://doi.org/10.1093/nar/gkx973. PMid: 29126202.
[33] Kitts PA, Church DM, Thibaud-Nissen F, et al. Assembly: A resource for assembled genomes at NCBI. Nucleic Acids Res 2016;44(D1):D73–80. https://doi.org/10.1093/nar/gkv1226. PMid: 26578580.
[34] Gill RM, Mehra V, Milford E, et al. Short SULF1/SULF2 splice variants predominate in mammary tumours with a potential to facilitate receptor tyrosine kinase-mediated cell signalling. Histochem Cell Biol 2016;146:431–44. https://doi.org/10.1007/s00418-016-1454-3. PMid: 27294358.
[35] Brassart-Pasco S, Brézillon S, Brassart B, et al. Tumor microenvironment: Extracellular matrix alterations influence tumor progression. Front Oncol 2020;10:397. https://doi.org/10.3389/fonc.2020.00397. PMid: 323518780.
[36] Piera-Velazquez S, Mendoza FA, Addya S, et al. Increased expression of interferon regulated and antiviral response genes in CD31+/CD102+ lung microvascular endothelial cells from systemic sclerosis patients with end-stage interstitial lung disease. Clin Exp Rheumatol 2021;39(6):1298–306. https://doi.org/10.55563/clinexprheumatol/ret1kg. PMid: 33253099.
[37] Shi Y, Xu Y, Xu Z, et al. TKI resistant-based prognostic immune related gene signature in LUAD, in which FSCN1 contributes to tumor progression. Cancer Lett 2022;532:215583. https://doi.org/10.1016/j.canlet.2022.215583. PMid: 35149175.
[38] Li X, Hou L, Zhang L, et al. OAS3 is a co-immune biomarker associated with tumour microenvironment, disease staging, prognosis, and treatment response in multiple cancer types. Front Cell Dev Biol 2022;10:815480. https://doi.org/10.3389/fcell.2022.815480. PMid: 35592250.
[39] Wang Y, Hu Y, Chen L, et al. Molecular mechanisms and prognostic markers in head and neck squamous cell carcinoma: A bioinformatic analysis. Int J Clin Exp Path 2020;13(3):371–81. PMid: 32269674.
[40] Kryczka J, Boncela J. Integrated bioinformatics analysis of the hub genes involved in irinotecan resistance in colorectal cancer. Biomedicines 2022;10(7):1720. https://doi.org/10.3390/biomedicines10071720. PMid: 35885025.
[41] Ying L, Zhang F, Pan X, et al. Complement component 7 (C7), a potential tumor suppressor, is correlated with tumor progression and prognosis. Oncotarget 2016;7(52):86536–46. https://doi.org/10.18632/oncotarget.13294. PMid: 27852032.
[42] Lu S, Peng L, Ma F, et al. Increased expression of POSTN predicts poor prognosis: A potential therapeutic target for gastric cancer. J Gastrointest Surg 2023;27(2):233–49. https://doi.org/10.1007/s11605-022-05517-4. PMid: 36451060.
[43] Chae J, Choi J, Chung J. Polymeric immunoglobulin receptor (pIgR) in cancer. J Cancer Res Clin Oncol 2023;149(19):17683–90. https://doi.org/10.1007/s00432-023-05335-4. PMid: 37897659.
[44] Huo X, Wang S, Song H, et al. Roles of major RNA adenosine modifications in head and neck squamous cell carcinoma. Front Pharmacol 2021;12:779779. https://doi.org/10.3389/fphar.2021.779779. PMid: 34899345.
[45] Ni H, Sun H, Zheng M, et al. Mining database for the expression and clinical significance of STAT family in head and neck squamous cell carcinomas. Transl Oncol 2021;14(1):100976. https://doi.org/10.1016/j.tranon.2020.100976. PMid: 33395750.
[46] Drappier M, Michiels T. Inhibition of the OAS/RNase L pathway by viruses. Curr Opin Virol 2015;15:19–26. https://doi.org/10.1016/j.coviro.2015.07.002. PMid: 26231767.
[47] Li Y, Banerjee S, Wang Y, et al. Activation of RNase L is dependent on OAS3 expression during infection with diverse human viruses. PNAS 2016;113(8):2241–6. https://doi.org/10.1073/pnas.1519657113. PMid: 26858407.
[48] Sabatini ME, Chiocca S. Human papillomavirus as a driver of head and neck cancers. Br J Cancer 2020;122(3):306–14. https://doi.org/10.1038/s41416-019-0602-7. PMid: 31708575.
[49] Yang E, Li MM. All about the RNA: Interferon-stimulated genes that interfere with viral RNA processes. Front Immunol 2020;11:605024. https://doi.org/10.3389/fimmu.2020.605024. PMid: 33362792.
[50] Berinde GM, Socaciu AI, Socaciu MA, et al. Thyroid cancer diagnostics related to occupational and environmental risk factors: An integrated risk assessment approach. Diagnostics 2022;12(2):318. https://doi.org/10.3390/diagnostics12020318. PMid: 35204408.
[51] Wu H, Eckhardt CM, Baccarelli AA. Molecular mechanisms of environmental exposures and human disease. Nat Rev Genet 2023;24(5):332–44. https://doi.org/10.1038/s41576-022-00569-3. PMid: 36717624.
[52] Meier MJ, Harrill J, Johnson K, et al. Progress in toxicogenomics to protect human health. Nat Rev Genet 2025;26(2):105–22. https://doi.org/10.1038/s41576-024-00767-1. PMid: 39223311.
[53] Li N, Wang J, Zhang N, et al. Cross-talk between TNF-α and IFN-γ signaling in induction of B7-H1 expression in hepatocellular carcinoma cells. Cancer Immunol Immunother 2018;67(2):271–83. https://doi.org/10.1007/s00262-017-2086-8. PMid: 29090321.
[54] Zheng Y, Li Y, Lian J, et al. TNF-α-induced Tim-3 expression marks the dysfunction of infiltrating natural killer cells in human esophageal cancer. J Transl Med 2019;17(1):165. https://doi.org/10.1186/s12967-019-1917-0. PMid: 31109341.
[55] Brasil da Costa FH, Lewis MS, Truong A, et al. SULF1 suppresses Wnt3A-driven growth of bone metastatic prostate cancer in perlecan-modified 3D cancer-stroma-macrophage triculture models. PLoS One 2020;15(5):e0230354. https://doi.org/10.1371/journal.pone.0230354. PMid: 32413029.
[56] Ouyang Q, Liu Y, Tan J, et al. Loss of ZNF587B and SULF1 contributed to cisplatin resistance in ovarian cancer cell lines based on Genome-scale CRISPR/Cas9 screening. Am J Cancer Res 2019;9(5):988–98. PMid: 31218106.
[57] Yang Y, Ahn J, Edwards NJ, et al. Extracellular Heparan 6-*O*-endosulfatases SULF1 and SULF2 in head and neck squamous cell carcinoma and other malignancies. Cancers 2022;14(22):5553. https://doi.org/10.3390/cancers14225553. PMid: 36428645.
[58] Musumeci G, Castrogiovanni P, Barbagallo I, et al. Expression of the OAS gene family is highly modulated in subjects affected by juvenile dermatomyositis, resembling an immune response to a dsRNA virus infection. Int J Mol Sci 2018;19(9):2786. https://doi.org/10.3390/ijms19092786. PMid: 30227596.
[59] Choi UY, Kang J-S, Hwang YS, et al. Oligoadenylate synthase-like (OASL) proteins: Dual functions and associations with diseases. Exp Mol Med 2015;47(3):e144. https://doi.org/10.1038/emm.2014.110. PMid: 25744296.
[60] Shaath H, Vishnubalaji R, Elkord E, et al. Single-cell transcriptome analysis highlights a role for neutrophils and inflammatory macrophages in the pathogenesis of severe COVID-19. Cells 2020;9(11):2374. https://doi.org/10.3390/cells9112374. PMid: 33138195.
[61] Zhang Y, Yu C. Prognostic characterization of OAS1/OAS2/OAS3/OASL in breast cancer. BMC Cancer 2020;20(1):575. https://doi.org/10.1186/s12885-020-07034-6. PMid: 32560641.